East European Journal of Physics. 2. 99-110 (2024)
DOI:10.26565/2312-4334-2024-2-08 ISSN 2312-4334

A SIMPLISTIC ANALYTICAL MODEL FOR HYDROGEN SURFACE COVERAGE UNDER THE INFLUENCE OF VARIOUS SURFACE-RELATED PROCESSES AND ION BOMBARDMENT

Ivan I. Okseniuk*, Viktor O. Litvinov, Dmytro I. Shevchenko, Inna O. Afanasieva, Valentyn V. Bobkov
V.N. Karazin Kharkiv National University, 4, Svobody Sq., Kharkiv, 61022, Ukraine
**Corresponding Author, e-mail: ivanokseniuk@karazin.ua*
Received April 1, 2024; revised April 22, 2024; accepted May 7, 2024

The paper describes a simple analytical model that allows the calculation of hydrogen surface coverage under the influence of several processes that can co-occur during the ion-beam bombardment/sputter analysis of a sample surface, in particular during analysis by secondary ion mass spectrometry (SIMS). The model considers processes of dissociative adsorption, desorption, absorption from the surface into the sample volume, and removal by ion bombardment. After describing the model, we provide some examples of its practical applications for interpretation of the experimental results obtained during *in situ* SIMS studies of hydrogen interaction with the hydrogen-storage alloys TiFe, Zr_2Fe, and with nickel. In the examples, some quantitative characteristics of surface-related processes involving hydrogen, such as hydrogen sputtering rate, activation energy of hydrogen desorption and absorption, have been successfully determined using various model approaches.
Keywords: *Secondary ion mass spectrometry; Hydrogen storage; Sputtering; Adsorption; Desorption; Ion bombardment; Kinetics*
PACS: 34.35.a, 68.43.–h, 68.49.Sf, 79.20.Rf

1. INTRODUCTION

Among rather few other surface analysis techniques, secondary ion mass spectrometry (SIMS) is capable of direct detection and imaging of hydrogen isotopes with high sensitivity. Hydrogen analysis with SIMS can sometimes be complicated by the occurrence of such processes as adsorption of hydrogen-containing molecules on the surface, diffusion, segregation, and desorption of hydrogen directly during the analysis [1–9]. Although the ease of occurrence of such processes constitutes an obstacle for hydrogen quantification and localization, it can be exploited to study those processes themselves since they are of great importance in certain fields: hydrogen interaction with hydrogen-storage materials [10] being one of such fields.

In our previous studies [11–15] of the interaction of hydrogen-storage alloys with hydrogen and oxygen using SIMS, it was found that the emission intensity of hydrogen-containing secondary ions can be used to monitor the presence and changes in concentration of hydrogen on the surface in a fairly wide range of experimental conditions. In earlier studies [16–19], SIMS had been already utilized to determine the characteristics of hydrogen interaction with metals. Papers [12,13,16–18,20] exemplify that the SIMS technique indeed provides good opportunities for *in situ* characterization of hydrogen interaction processes with metals and alloys.

However, difficulties in the analysis of such experimental results arise when several processes affecting hydrogen concentration on the surface occur simultaneously during the measurements. Therefore, to understand how hydrogen surface concentration is affected by the action and characteristics of each such process, an analytical model was developed that considers the influence of several processes that can occur within the range of experimental conditions of SIMS studies [12,13]. The analysis with the developed model allows distinguishing and predicting (to a certain extent) the results of action of each process, which, ultimately, provides grounds for appropriate interpretation of the experimental results.

The model considers processes of hydrogen dissociative adsorption, recombinative desorption, dissolution/absorption from surface chemisorption sites into the bulk, and processes of ion beam removal/sputtering. One quite commonly occurring process, that we omitted from consideration in the model, is hydrogen segregation on the surface. To include the surface segregation, hydrogen in the bulk has to be considered and characterized, which is generally a rather complex task when real samples (apart from near perfect single-crystals) are studied [2,4,5,21,22]. In our studies, the samples are usually polycrystalline alloys, often with complex constitution and numerous uncharacterized bulk defects/features what may influence hydrogen in the bulk. Other than our SIMS instrument we don't have other means to characterize bulk-hydrogen at small concentrations (as relevant for our experimental conditions), and without having the details about bulk hydrogen we don't attempt describing it. Therefore, the model considers only a comparably small presence of bulk hydrogen and its appearance on the surface mainly as a result of the ion beam etching of the sample. A very limited approach to segregation is described in **Section 3.5**.

Although the model was intended mainly to help with *in situ* SIMS studies of hydrogen interaction with a sample as exemplified in **Section 3**, recent studies [23–25] reported that the use of H_2 flooding might be also beneficial in SIMS multilayer depth profiling and elemental quantification. In such measurements the balance between hydrogen adsorption

Cite as: I.I. Okseniuk, V.O. Litvinov, D.I. Shevchenko, I.O. Afanasieva, V.V. Bobkov, East Eur. J. Phys. 2, 99 (2024), https://doi.org/10.26565/2312-4334-2024-2-08

and beam-etching will be of main focus although other processes can co-occur as well, therefore the usage of such a model can be fruitful in this application. Besides that, the model may also have some relevance for vacuum devices operation where hydrogen adsorption and desorption from surfaces are important factors affecting vacuum conditions and operation. In particular, accelerators and plasma devices have surfaces exposed to energetic irradiation by ions, electrons, or photons. If in accelerators the ion-stimulated desorption is a known and actively studied issue [26], there are plasma devices for which irradiation-stimulated hydrogen desorption is an essential part of their operation [27–29]. Recently, a similar but much more sophisticated and material-specific model was developed for hydrogen interaction with tungsten in relevance to magnetic confinement plasma fusion devices [30]. For such applications, the presented here model, one way or another, has to be complemented by an appropriate consideration of hydrogen within the solid's bulk.

2. DESCRIPTION OF THE MODEL

2.1. Main Model Equation and Processes Representation

The basis of the model is an equation that establishes the relation of the hydrogen concentration changes on surface over time under the influence of a number of possible processes. Each considered process has its representative term in equation (1).

$$\frac{d\theta}{dt} = 2aF(1-\theta)^2 - 2b\theta^2 - D\theta - s_1 j_p \theta - 2s_2 j_p \theta^2 + s_0 j_p \theta_0. \quad (1)$$

Here $\theta = c_H/c_{Hmax}$ is the relative coverage of the surface by chemisorbed hydrogen atoms, defined as a ratio of the hydrogen concentration (c_H) to a certain maximal value of the concertation (c_{Hmax}).

The first term is responsible for the increase of coverage due to dissociative adsorption of hydrogen molecules. It takes into account the decrease in the sticking coefficient with increasing coverage $(1-\theta)^2$ [31], which arises from the necessity for two unoccupied adsorption sites according to Langmuir's model of dissociative adsorption of diatomic molecules. a is the initial sticking probability, F is the flow of hydrogen molecules into the area of one adsorption site. F is calculated by:

$$F = \frac{1}{n_{at}} \times \frac{p_{H2}}{\sqrt{2\pi m_{H2} k_B T_{H2}}}, \quad (2)$$

where p_{H2} is hydrogen partial pressure near the sample surface, n_{at} is the density of hydrogen adsorption sites on the surface. It is commonly assumed that n_{at} is roughly equal (it may differ by 2-3 times) to the density of substrate surface atoms. m_{H2} is the mass of a hydrogen molecule, T_{H2} is the hydrogen gas temperature, k_B is Boltzmann constant. If the presence of surface roughness is presumed, a coefficient-multiplier should be introduced for this term (and, perhaps, for the other terms too).

The second term of equation (1) is responsible for removing hydrogen from the surface by thermally-stimulated recombinative desorption. Hence, b is the rate coefficient of desorption, which in the simplest form can be described similarly to the Polyani-Wigner equation, widely used in the temperature-programmed desorption (TPD) analysis. So b can be expressed as:

$$b = \frac{b_0}{2} \exp\left\{\frac{-E_a}{RT}\right\}, \quad (3)$$

where $b_0/2$ is the pre-exponential factor, E_a is the activation energy of desorption, T is the sample temperature.

The next term ($-D\theta$) describes the dissolution/absorption of hydrogen from the surface into the bulk of the sample. Accordingly, D is the frequency of hydrogen atoms absorption from the surface into the volume. In our experimental SIMS practice, some diffusion of hydrogen atoms from the outmost surface layer inward of the sample occurred for practically every studied intermetallic alloy: $LaNi_5$ and its Al-, Mn-modified variants [32], TiFe [12], Zr-based non-evaporable getter alloys [13]. The degree of such absorption below the surface was different based on alloy characteristics. For three Zr-based alloys, the absorbed amount was roughly proportional to hydrogen exposure ($p\{H_2\}\times t$), was seemingly unlimited at studied hydrogen pressures (below 10^4 Torr, 1 Torr = 133.322Pa), and was regarded as true bulk-absorption. For other studied alloys, only a limited amount of hydrogen migrated to subsurface. Estimated amount of such subsurface-migrated hydrogen was comparable to or few times higher than the amount of surface-chemisorbed hydrogen, and it could not be increased by increasing hydrogen exposure. Such limited absorption was characteristic to the alloys which had relatively small enthalpies of their hydrides or hydrogen solid solution, which equilibrium pressure are of order of the atmospheric pressure that is many orders of magnitude higher than the studied $p\{H_2\}$ range. Whereas, Zr-based getter alloys which absorbed hydrogen in bulk are characterized by large-value negative enthalpies, resulting in the high stability of hydrides/dissolved hydrogen at room temperature-UHV conditions. For most of the alloys dissolution/migration rate increased with temperature indicating the presence of the activation barrier.

The following two terms ($-s_1 j_p \theta$ and $-2s_2 j_p \theta^2$) describe the removal of hydrogen from the surface as a result of ion beam bombardment. Therefore, these terms are proportional to the ion beam current density (j_p). The term $-s_1 j_p \theta$ represents all mechanisms of ion beam induced removal the rate of which is proportional to hydrogen coverage: collision cascade sputtering would be one of such mechanisms. The term $-2s_2 j_p \theta^2$ represents the removal by ion beam induced

recombinative desorption (i.e. in the form of H_2 molecules), therefore it is proportional to hydrogen coverage squared: such removal may occur at high hydrogen coverage since the energy needed to form and remove an H_2 molecule from the surface is substantially smaller than the energy needed to remove an alone H atom. The coefficients s_1 and s_2 represent the effectiveness of the corresponding removal rates.

Regarding the ion beam sputtering of hydrogen, the authors of paper [33] provided theoretical argumentation for ineffectiveness of the collision cascade sputtering in the case of chemisorbed hydrogen atoms on the surface of metals. According to the argumentation, the amount of kinetic energy transferred to a hydrogen atom in a collision with a metal atom having typical values of the kinetic energy in the cascade is not enough to overcome the bonding of hydrogen atom to the surface. The transferred energy is reduced due to the large mass difference between hydrogen and metal atoms. However, the experimental findings about the ion beam removal rates of chemisorbed hydrogen at small surface coverages indicate that the rate of hydrogen removal is instead 20-30% higher than the removal rate of chemisorbed oxygen[2] [12], and these rates are practically of the same order as the sputtering rate of metal atoms. Such rather high effectiveness of hydrogen removal may be a result of hydrogen sputtering in the form of molecules MeH formed with sputtered metal atoms Me, as proposed for the case of sputtering of oxygen-metal systems [34]. In such a case, there is no need to transfer the kinetic energy to hydrogen atoms to detach them from the surface, instead, hydrogen atoms only need to replace the bond with the surface by a bond with a metal atom that leaves the surface during a sputtering event. Known data indicate [35] that the binding energy values are comparable for the case of hydrogen atoms on metal surfaces and for the case of hydrogen atoms within a molecule with a metal atom. The existence of such a mechanism is confirmed by the presence of hydrogen molecules with metal and semiconductor atoms in the mass spectra of neutral sputtered particles from surfaces with the hydrogen presence [36,37], and also confirmed by the presence of polyatomic hydrogen-containing secondary ions in the mass spectra obtained in [11–14].

Regarding the removal of hydrogen by recombinative desorption of H_2 molecules induced by ion bombardment, such a removal may occur within very short time after an ion impact on the surface as a result of electrons excitation around the impact place. Such electronic excitations (if ~10 keV ions can induce them) are known [38,39] to desorb hydrogen molecules from surfaces including surfaces that adsorb hydrogen dissociatively, although such desorption can deviate from the second-order kinetics [38,39]. Another pathway of ion-induced H_2 desorption might be provided at the 'late' stages of collision cascades. At these stages, the energy of an impacting ion becomes distributed among many target atoms in the vicinity of the impact, and although individual atoms no longer have enough energy for knock-off sputtering, the activation energy of the order of 1 eV may still be supplied for associative desorption of H_2 molecules. Studies [40,41] show that the 'effective temperature' of the near-surface region excited by an impact of ions with the energy of an order of 10 keV can reach thousands of K, which can promote the thermal-like hydrogen desorption.

The last term $s_0 j_p \theta_0$ introduces the hydrogen contained in the sample volume and its appearance on the surface as a result of the sample material removal by ion beam sputtering, i.e. as a result of sample erosion/etching and gradual 'shifting' of the surface into the depth of the sample. Small amount of homogeneously distributed immobile hydrogen in the sample bulk is assumed by this term. If $s_0 j_p$ represents the frequency of ion beam removal of one monolayer of the sample atoms then θ_0 represents the coverage-equivalent hydrogen content per one monolayer in the sample volume.

2.2. The Steady State Solution

Under conditions of dynamic equilibrium, i.e. when hydrogen concentration on the surface is constant, the sum of all components in (1) is zero. Considering all process rate constants as independent of time and coverage, expression (1) is a quadratic equation for θ. Therefore, it is possible to obtain a solution (4) that expresses the coverage dependence on all coefficients present in (1).

$$\theta = \frac{D+4aF+s_1 j_p - \sqrt{(D+4aF+s_1 j_p)^2+8(b-aF+s_2 j_p)(2aF+s_0 j_p \theta_0)}}{4(-b+aF-s_2 j_p)}. \tag{4}$$

If there is no absorption into the bulk ($D = 0$) and also there is no thermally-stimulated desorption ($b = 0$), expression (4) can be rewritten as:

$$\theta = \frac{4a\frac{F}{j_p}+s_1 - \sqrt{8a\frac{F}{j_p}(s_1+2s_2-s_0\theta_0)+s_1^2+8s_2 s_0 \theta_0}}{4a\frac{F}{j_p}-4s_2}, \tag{5}$$

in which, the current density of the ion beam and hydrogen partial pressure are present only in a form of the ratio F/j_p. That is, if an x-fold change in the current density is accompanied by the same x-fold change in the hydrogen partial pressure, then the coverage remains unchanged. Such a result was indeed obtained more than once for some of the studied alloys [12,13] if not heated.

[2] Note that the mass of oxygen atoms is only several times smaller than the mass of metal atoms, not dozen times smaller as in the case of hydrogen atoms.

2.3. Calculated Effects of Different Processes on Steady State Surface Coverage

Fig. 1 (**a-d**) shows the dependences of surface coverage on hydrogen pressure, as calculated using expression (4). To illustrate the influence of various processes, calculations were done with a set of parameters values that characterize the processes included in equation (4). Fig. 1**a** shows how the residual/bulk hydrogen concentration affects the coverage dependence on hydrogen pressure.

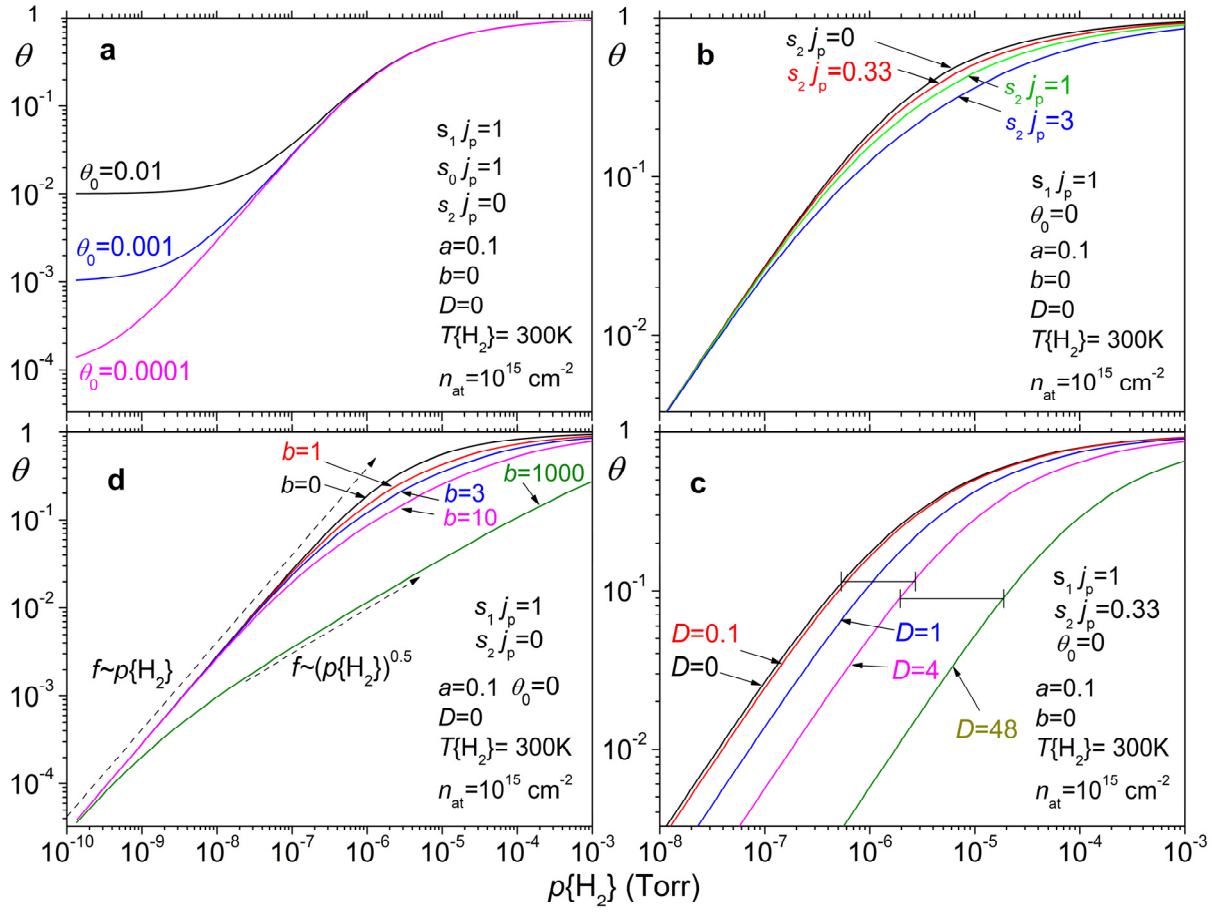

Figure 1. The dependences of surface coverage by adsorbed hydrogen atoms on the hydrogen gas pressure as calculated using expression (4) for a set of values of the parameters that characterize the processes included in the model. **a**: influence of the residual hydrogen presence, **b**: influence of the ion-induced recombinative desorption, **c**: influence of the absorption rate from the surface into the bulk, **d**: influence of the rate of thermally-stimulated recombinative desorption.

Fig. 1**b** illustrates how the rate of hydrogen removal by ion-induced recombinative desorption influences the coverage dependence on pressure. The influence of ion-induced desorption manifests as a decrease of the rate with which the concentration increases: It slows down the asymptotic approaching to 'the saturation', but its influence diminishes at low coverages due to the second order kinetics of the desorption.

The main effect of the presence of absorption from surface to bulk is the decrease in surface coverage at the same hydrogen pressure (Fig. 1**c**). As the rate of absorption increases, the dependence curves shift toward higher pressures, since to achieve a certain concentration, the part of hydrogen which is removed from the surface due to absorption must be compensated by an increase in the amount of adsorbed hydrogen, which is achieved when the pressure is increased.

The influence of the rate of thermally-stimulated desorption is illustrated in Fig. 1**d**. Relatively small values of the desorption rate produce the effect which has been already described above in the explanation for Fig. 1**b**. However, the values of the desorption rate at high temperatures can be very large compared to the ion sputtering rate (the curve for b=1000 in Fig. 1d is an example). In such a case, the dependence of coverage on the pressure at middle-to-small coverages becomes proportional to the square root of the pressure instead of the linear dependence on the pressure, which is in accordance with Sievert's law. This change from the linear to the square root dependence can be used to identify the recombinative desorption process when it dominates over other hydrogen removal processes.

3. PRACTICAL APPLICATIONS IN SIMS MEASUREMENTS

The main aim of the development of the model was its application for interpretation of experimental results of hydrogen interaction with alloys or metals obtained during *in situ* SIMS measurements. Therefore, practical application of the model for processes analysis as well as for obtaining quantitative estimates of the characteristics of hydrogen interaction with few studied samples are described below.

3.1. A Time-Dependent Solution Characterizing Ion Beam Sputtering

At low coverages, the rate coefficient of linear hydrogen removal by ion bombardment $j_p s_1$ can be determined experimentally. In the absence of desorption (b=0), the other terms in (1) proportional to θ^2 can be neglected at low coverages. Besides that, if there is no absorption into the bulk (D=0), then equation (1) can be simplified to the form:

$$\frac{d\theta}{dt} = -\theta\left(4aF + s_1 j_p\right) + 2aF + s_0 j_p \theta_0. \tag{6}$$

If only θ depends on time, then the solution of (6) is:

$$\theta = C_0 \exp\left\{-\left(4aF + s_1 j_p\right)t\right\} + \frac{2aF + s_0 j_p \theta_0}{4aF + s_1 j_p}. \tag{7}$$

At low adsorption rates (at low hydrogen pressures) compared to the sputtering rate, expression (7) can be represented in the form:

$$\theta \approx C_0 \exp\left\{-s_1 j_p t\right\} + C_1, \tag{8}$$

that is, in the form of an exponential decay function, where C_0+C_1 is the initial value of the coverage at the beginning of sputtering, while C_1 is the residual coverage after prolonged sputtering. Using this function for fitting the dependences of H^- emission intensity on time measured during the sputtering of the chemisorbed hydrogen that was beforehand adsorbed at small exposures (<0.3 Langmuir), it is possible to determine the value of $s_1 j_p$, or the value of characteristic removal time $\tau = (s_1 j_p)^{-1}$, as shown in Fig. 2.

It should be noted that it is potentially possible to experimentally characterize also the quadratic removal rate $s_2 j_p$ in similar experiments if the coverage (exposure) is not limited to low amounts but extended to the saturation. However, the experiment results with the TiFe and few other alloys indicated that some amount of hydrogen can diffuse into subsurface sites or into the bulk, and this diffusion is facilitated by sample temperature or by high surface coverage [13,14,32]. Therefore, in such cases, the assumption that hydrogen is adsorbed only within the topmost surface monolayer is not valid anymore. Another possible complication is the nonlinearity of secondary ion yield relation to hydrogen coverage [12]. Due to these factors, the analysis of hydrogen removal was not attempted at high coverages.

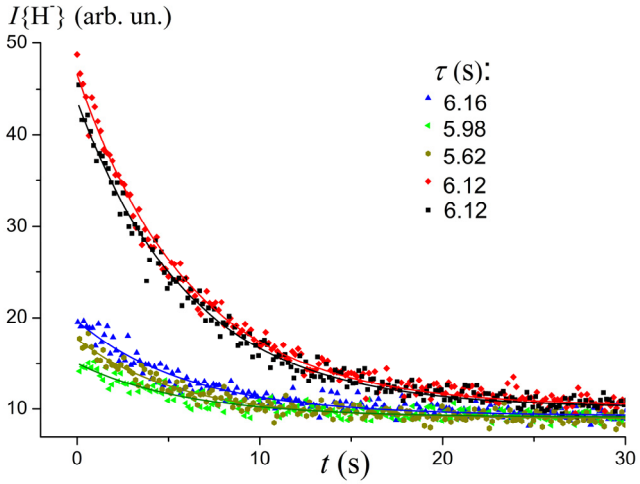

Figure 2. Points: dependences of the emission intensity of H^- secondary ions on sputtering time as measured after various small exposures of the TiFe alloy surface in hydrogen atmosphere. **Lines**: curves of the exponential decay function (8) used to approximate the measured dependences. The values of characteristic removal time τ obtained from the approximations are also listed.

3.2. Applications for Adsorption, Sputtering, and Desorption Characterization

Fig. 3 shows examples of the approximations of experimental data using expressions (2-4) for the dependences of hydrogen-containing secondary ions emission intensity on hydrogen pressure (Fig. 3**a**) and the sample temperature (Fig. 3**b**) which were measured with the TiFe alloy sample. Fig. 3**a** shows the measured points and the fitting curves for two types of secondary ions: $^{48}TiH^+$ and H^-. The corresponding values of adsorption and sputtering parameters determined from their approximations are also listed. To compare the emission intensities of the secondary ions with the amount of hydrogen coverage, the correspondence of θ = 1 to intensity values of ~7700 relative units was used for $^{48}TiH^+$ and ~600 relative units for H^-. Such values were determined by measuring the intensities after high (>10^4 Langmuir) surface exposures in hydrogen atmosphere without ion bombardment just after the beginning of bombardment. The ion bombardment was initiated with substantially reduced beam current density to minimize hydrogen removal, thus appropriate normalization of intensity values using the ratio between the nominal and the reduced beam current densities was done.

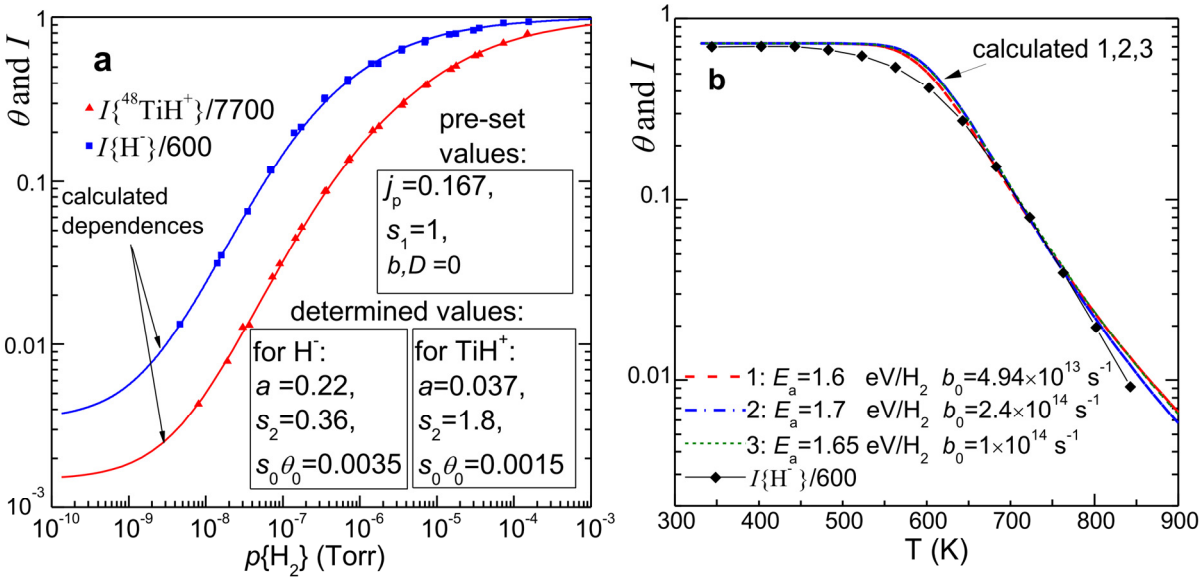

Figure 3. Approximations of the measured dependences for the TiFe alloy. **a**: secondary ion emission intensity dependences $I\{^{48}TiH^+\}$ and $I\{H^-\}$ on hydrogen pressure and their fits using formula (4), **b**: $I\{H^-\}$ dependence on the sample temperature at hydrogen pressure $p\{H_2\}=7.1\times10^{-6}$ Torr and its fits using formulae (2-4), (assuming D=0).

Besides the intensity scale factors, other pre-set parameters in the approximations were the rate coefficient of hydrogen removal: $s_1 j_p = 0.167$ s^{-1} as determined from the results shown in Fig. 2, and the value $n_{at} = 1.8\times10^{15}$ cm^{-2} used in expression (2) (it was calculated using the density of TiFe alloy 6.5 g×cm^{-3} [42]), assuming that it is equal to the density of possible hydrogen atom chemisorption sites on the alloy surface. Other parameters values included in equation (4), namely the sticking probability, the rate coefficient of ion-stimulated H_2 desorption, the contribution of hydrogen content in the sample bulk to the surface coverage, were determined when approximating the measured dependences on hydrogen pressure by formula (4), as shown in Fig. 3**a**, provided that absorption (D=0) and desorption (b=0) are effectively absent.

The parameters values determined by the approximation differ quite substantially when using $I\{^{48}TiH^+\}$ or $I\{H^-\}$ dependences. Nevertheless, both values of the sticking probability correspond to the range of typical values for many transition metals [35,43]. The relatively large value of s_2/s_1 determined from the approximation using $I\{^{48}TiH^+\}$ may indicate that, starting from the coverage $\theta \geq 0.278$, most of the hydrogen is removed from the surface by ion-stimulated recombinative desorption.

The difference in the measured pressure dependences for TiH^+ and H^- is because the yields of secondary ions either TiH^+ or H^- (or both of them) nonlinearly depend on the hydrogen surface concentration when the concentration is high. The possible reasons for the nonlinearity are discussed in [12]. Since the secondary ion emission intensity values corresponding to the coverage saturation (7700 rel. units for TiH^+ and 600 rel. units for H^-) were determined at 'maximal' coverage, the nonlinearity is included in the dynamic range of the ion emission intensity and therefore affects the values resulting from the fittings, including the residual hydrogen concentration (θ_0) and sticking probability (a), even that the dependence lines for $I\{TiH^+\}$ and $I\{H^-\}$ in Fig. 3**a** are parallel (can match each other when shifted) at low concentrations. Unfortunately, it is not possible to determine whether the yield dependences of these secondary ions on the concentration are linear or not with the available experimental data. In order to obtain reliable parameters values by doing such approximations as shown in Fig. 3, the knowledge of the exact relationship between the secondary ion emission intensities and the hydrogen concentration is required. To obtain such knowledge, it is necessary either to know the value of the sticking probability of hydrogen and its precise dependence on coverage or to use another quantitative method for in situ calibration, such as temperature programmed desorption (TPD) or nuclear reaction analysis (NRA) [16,17,44–46].

Fig. 3**b** shows the measured points of the temperature dependence of secondary ion emission intensity and several variants of their approximation using expressions (2-4) in the presence of thermally-stimulated hydrogen desorption from the surface. The values of the desorption activation energy E_a and the pre-exponential factor b_0 are also given for each approximation variant. At coverages $\theta \leq 0.2$, the calculated dependences of the coverage on the temperature coincide quite well with the measured points. However, at higher coverages, experimental results indicate that desorption begins at significantly lower temperatures than predicted by the calculations. Most probably this is a result of a reduction of the desorption activation energy at high coverages, which has not been accounted for in (3). This reduction may be related to the desorption from less strongly bound states on the surface, or related to the existence of repulsive interaction between the adsorbed hydrogen atoms [47–49]. Another problem concerning specifically the approximation in Fig. 3**b** is the presence of a 'compensation effect' [47,50], which consists in that different combinations of the values of desorption activation energy E_a and of the pre-exponential factor b_0 produce very similar calculated desorption rate dependences. The accuracy of the experimental data, therefore, allows fitting the data by a certain range of different combinations of E_a and b_0, as illustrated by curves 1-3. In addition, possible non-linearity of the secondary ion yield relation to the coverage

can also contribute to the mismatch of desorption rate at high coverages. Thus, unfortunately, in the absence of an accurately calibrated relation between the ion yield and hydrogen coverage/concentration, the estimates of the parameters obtained with the approximations in Fig.3 are not reliable.

3.3. Constant-Coverage Approach to Characterize Thermally-Activated Desorption Process

A possible approach that can bypass the mentioned earlier 'compensation effect' and determine the value of the desorption activation energy separately is realized by setting up the desorption experiment in the constant coverage mode. The calibration of secondary ion yield is also unnecessary unless the activation energy needs to be tied to a specific coverage value. Although, one should make sure the relationship between the ion yield and hydrogen concentration on the surface is not affected by the sample temperature.

When a dynamic equilibrium is established among the action of a number of processes, which results in a certain surface coverage by chemisorbed hydrogen, and when only the desorption rate coefficient depends on temperature[3], the hydrogen pressure near the surface can be expressed using relations (1-3) as follows:

$$p = c_1 \exp\left\{\frac{-E_a}{RT}\right\} + p_0, \tag{9}$$

where, E_a is the desorption activation energy, T is the surface temperature, c_1, p_0 are constants that depend on the coverage and the parameters values in (1-3). Formula (9) expresses the necessity to increase pressure exponentially with temperature in order to compensate for the increasing desorption rate while maintaining the same coverage.

The experiments testing such approach were performed with a polycrystalline nickel sample under experimental conditions similar to those described in [12]. During the experiments, hydrogen pressure was adjusted and measured following each stepwise increase of the sample temperature, in order to maintain constant coverage. The $^{58}Ni_2H^+$ emission intensity was used as the main indicator of coverage. The examples of the measured dependences of hydrogen gas pressure on the sample temperature are shown in Fig. 4**a**.

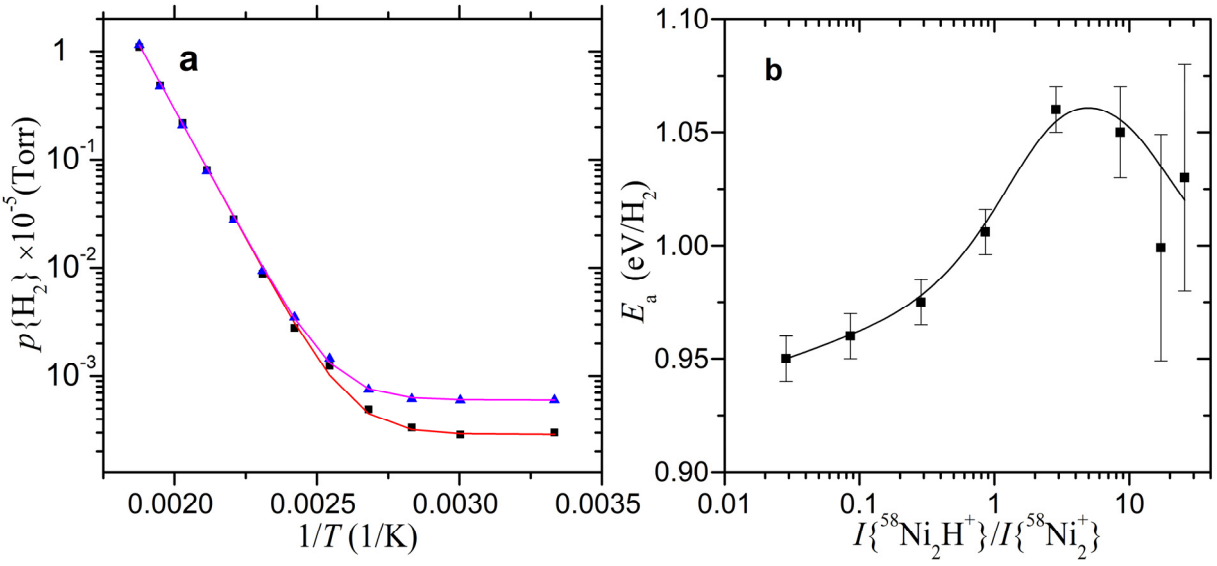

Figure 4. a: Dependences of the hydrogen gas pressure needed to maintain the same surface coverage with chemisorbed hydrogen on the reciprocal temperature of the nickel sample. Points denote experimental data, lines correspond to its fit with formula (9). **b**: Dependence of the obtained hydrogen desorption activation energy E_a on the ratio of secondary ion emission intensity $I\{^{58}Ni_2H^+\}/I\{^{58}Ni_2^+\}$, serving as a relative measure of the surface coverage with hydrogen.

The plotted two sets of data were obtained at twofold-different values of ion beam current density but the same coverage. The logarithmic scale plot of hydrogen pressure on the reciprocal sample temperature gives a straight line indicating the existence of exponential dependence in the temperature range where the desorption rate dominates over the ion-induced removal. Fitting the data (see the lines in Fig. 4**a**) with function (9) allows one to determine the desorption activation energy E_a. Such measurements and approximations were carried out at different hydrogen coverages, which thereby provided information on how E_a changes over about two orders of the coverage amount. Fig. 4**b** shows the dependence of E_a on the secondary ion emission intensity ratio $I\{^{58}Ni_2H^+\}$ / $I\{^{58}Ni_2^+\}$, which serves as an instrument-independent measure of the relative surface coverage by chemisorbed hydrogen [17,18]. The obtained values are close to the known values of E_a = 1 eV/H_2 for Ni(111), Ni(100) [43], whereas the increase of H_2 adsorption heat (which is related to the measured here E_a) from small to moderate coverages was also observed for Ni(110) [51].

[3] if there is effectively no absorption, and neither the rate of ion-induced hydrogen removal nor the chemisorption sticking probability depend on the sample temperature, which is valid for the TiFe alloy, at least in the range of 300-500 K [12]

3.4. Characterizing Thermally-Activated Absorption/Dissolution Processes

The developed model was also applied to characterize hydrogen absorption/dissolution process, i.e. the transition of hydrogen atoms from the surface chemisorbed sites into the volume of the Zr_2Fe getter alloy sample [13]. In the studies series with Zr_2Fe, the dependences of emission intensities of several types of negative secondary ions on hydrogen pressure were measured at three sample temperatures. The bombarding ion beam current density j_p was reduced fivefold from the nominal during those measurements. Such measured dependencies are shown in Fig. 5 for the secondary ions H^-, $^{56}FeH^-$, and $^{90}ZrH_2^-$. It was also found [13] that increasing the sample temperature above 300 K leads to a progressive increase in the efficiency of hydrogen absorption into the bulk of the alloy.

Following the model predictions, a substantial increase in the rate of hydrogen absorption from the surface into the depth of a sample causes a shift of the coverage dependence on the pressure towards higher pressures (Fig. 1**c**). Similar shift of the curves towards higher pressures is observed in the experimental results in Fig. 5 with increasing the sample temperature. For comparative purposes, the dependences measured at 513 K are additionally plotted in Fig. 5 with their hydrogen pressure values multiplied by 10 (hollow point symbols). These 'shifted' dependences approximately coincide with the dependences measured at 627 K, thus the dependences measured at 513 and 627 K are approximately parallel with ten times difference in the hydrogen pressure between them, which is similar to the parallel shifts predicted in Fig. 1**c**.

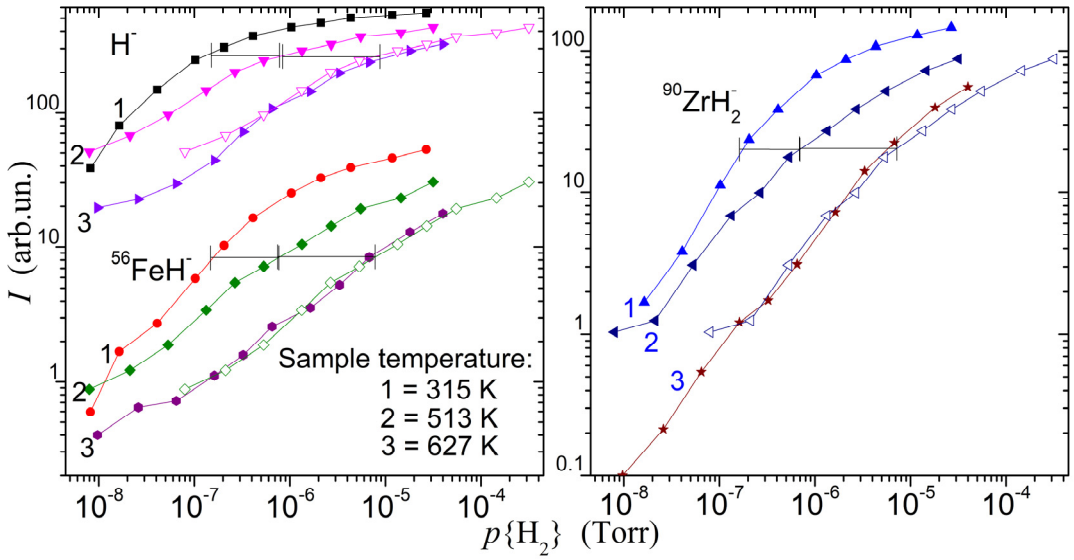

Figure 5. Dependences of the secondary ion emission intensity of negative hydrogen-containing secondary ions on hydrogen partial pressure measured at several temperatures of the Zr_2Fe alloy sample. For these measurements, the current density of the primary ion beam was fivefold-reduced ($s_1 j_p \sim 0.05$ s^{-1}) from its nominal value.

Considering that the absorption of hydrogen from the surface chemisorption states into the bulk of the alloy is a thermally-activated process, it is possible to estimate the effective value of its activation energy from the available experimental results. Besides the desorption, expression (9) can be used for the evaluation of the absorption activation energy too. The values of c_1, p_0, and E_a can be found after selecting three hydrogen pressure values at each sample temperature that correspond to the same coverage. At 315 K, the hydrogen coverage is mostly limited by the ion beam removal, and the rate of hydrogen outflow into the bulk is comparatively small [13], thus in expression (9), the contribution from p_0 is dominant. At 513 and 627 K, the rate of hydrogen removal from the surface by absorption already exceeds several times the rate of its sputtering by ion beam, thus in expression (9), the contribution of $c_1\exp\{-E_a/(RT)\}$ is dominant, which allows determining c_1 and E_a. The found value of the absorption activation energy is E_a=0.61 eV at hydrogen coverage around the middle of the investigated range. Since based on only three available points of hydrogen pressure it is impossible to confirm the presence of a straight-line segment on a logarithmic plot, similar to that in Fig. 4**a**, the found E_a value can be considered only as an estimate.

3.5. Characterizing the Surface Stage of Desorption of Bulk Absorbed Hydrogen

In such process, hydrogen atoms migrate from the volume of a metal/alloy to its surface (let's call it the bulk stage) where they recombine into H_2 molecules and desorb (the surface stage). The bulk stage can consist of other sub-stages such as H-detrapping, hydride phase decomposition, diffusion and we won't consider the details of the bulk stage due to its general complexity and our inability to control/study it with SIMS. The surface stage is assumed to be the same as for the desorption of chemisorbed hydrogen, although the exceptions from this are possible. The hydrogen atoms migrating from the bulk to the surface are 'segregating' on the surface before the desorption in the same states as chemisorbed hydrogen. Therefore, in SIMS conditions, the processes included in equation (1) apply. Essentially, the surface receives a flow of 'segregating' hydrogen atoms from the bulk. This flow, in one of most simple ways, can be modelled by a term (10) equivalent to atomic (first order) adsorption and be added to the equation (1).

$$+k_s(1-\theta). \tag{10}$$

Here k_s is the segregation frequency which depends on all of the bulk sub-stages, (1–θ) is the surface site availability factor. This process in isolation should produce increase of the coverage up to the saturation. In our SIMS experimental practice, it was never observed in isolation, but only simultaneously with other processes which makes it difficult to study. However, there had been experiments where it helped in studying the surface desorption stage.

Hydrogen absorbed in the bulk of the Zr_2Fe alloy could be desorbed by high-temperature heating of the sample. The desorption rate could be measured by gas mass spectrometer (TDS/TPD technique) and hydrogen coverage on the surface could be simultaneously monitored with H-containing secondary ion signal. Such experiments were presented in [13], although a round of similar experiments was conducted later with slightly modified technique. Briefly, in these experiments the sample was exposed to various hydrogen pressures for 175 seconds, at T ≈ 473 K. The Ar^+ beam bombardment was started simultaneously with heating of the sample to generate secondary ions for monitoring of hydrogen coverage changes on the surface. The intensity changes of ZrH^+ secondary ions and the hydrogen pressure in the sample chamber, reflecting desorption of the absorbed hydrogen during the temperature ramp (1.45 K/s) after exposures, are shown in Fig. 6.

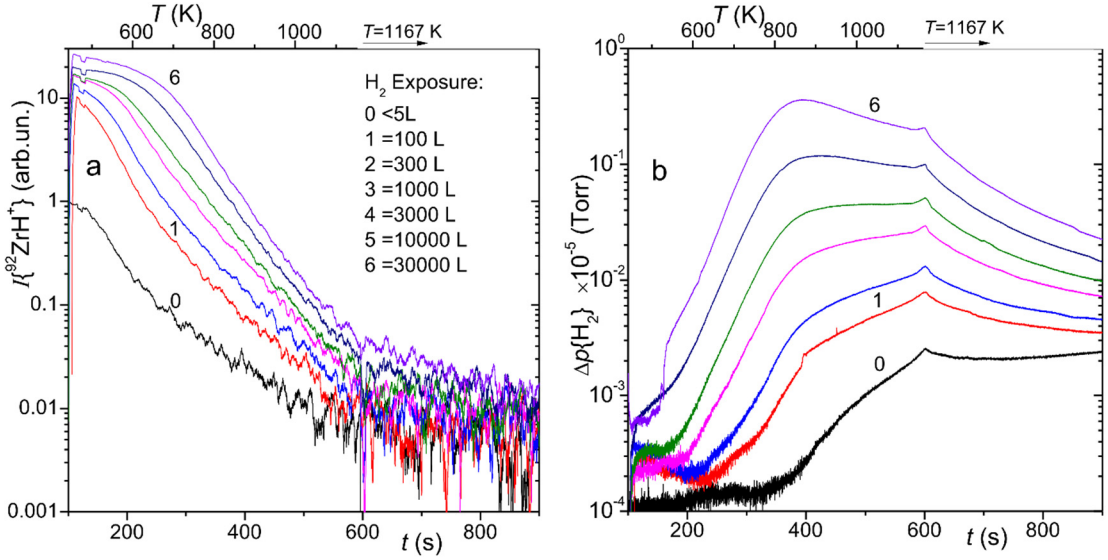

Figure 6. Dependences of emission intensity of $^{92}ZrH^+$ secondary ions on time (**a**) and dependences of hydrogen pressure in the sample chamber on time (**b**) during the heating and desorption of hydrogen from the Zr_2Fe alloy sample exposed to hydrogen atmosphere (exposures: <5 to 3×10^4 Langmuir). The $I\{^{92}ZrH^+\}$ dependences are smoothed by a moving average filter with a window size of 8 s for better visibility, and the background hydrogen pressure in the sample chamber is subtracted from the hydrogen pressure dependences.

During the analysis of these results, we hypothesized that in these experiments surface hydrogen coverage might be in an effective equilibrium between the segregation of hydrogen and hydrogen removal processes (its thermal desorption and sputtering by ion beam) since the surface was not saturated with hydrogen when substantial desorption occurred. At high temperatures, the rate of (thermal) recombinative desorption can be much higher than that of the beam sputtering. Therefore, the main processes that determine the hydrogen surface coverage are its segregation on surface and recombinative desorption, whereas impacts of other processes are comparably small. The segregation flow in such conditions is approximately equal to the desorption flow (when neglecting all other processes and neglecting the change of actual amount of hydrogen on the surface), hence the measured pressure rise due to the desorbing hydrogen $\Delta p\,\{H_2^{\text{desorb.}}\}$ can be used as a measure of the segregation flow. In the dynamic equilibrium corresponding to such conditions, from (1) we can find:

$$2b\theta^2 \approx C_2\Delta p\{H_2^{\text{desorb.}}\}, \tag{11}$$

where C_2 is an instrument-sample-characteristic constant. Relation (11) is similar to the main relation of conventional TDS-analysis for second order desorption, but the crucial difference here is that in case of the desorption from bulk Polyani-Wigner equation generally cannot be used to find the surface coverage. The relation (11) can also be expressed as

$$\frac{\Delta p\{H_2^{\text{desorb.}}\}}{\theta^2} \approx C_3 b, \tag{12}$$

where C_3 is another instrument-sample-characteristic constant. From the experiments in Fig.6, we have both the desorbing hydrogen pressure and ZrH^+ ion intensity which reflects the surface coverage. According to (12), the ratio

$\Delta p\{H_2^{desorb.}\}/(I\{ZrH^+\})^2$ should be proportional to the desorption frequency constant, which (if not dependent on coverage) should be a function of temperature only and, in these experiments, should be the same at the same sample temperature. The ratio is plotted versus desorption time/sample temperature in Fig. 7a. Indeed, the ratio curves constructed from different hydrogen absorption-desorption experiments coincide at higher temperatures, demonstrate seemingly exponential growth when the sample temperature increases linearly, and demonstrate plateau when temperature is stabilized at 1167K, which is the expected behavior for the desorption frequency constant. This validates the hypothesis and the assumptions above. Plotting the ratio curves using a logarithmic scale versus inverse temperature Fig. 7b produces a straight line in the region where the individual curves coincide, confirming the exponential dependence on temperature. Fitting the line with exponential function similar to (3) allows extraction of the activation energy E_a=1,85 eV of hydrogen desorption from the surface of the studied Zr_2Fe alloy sample.

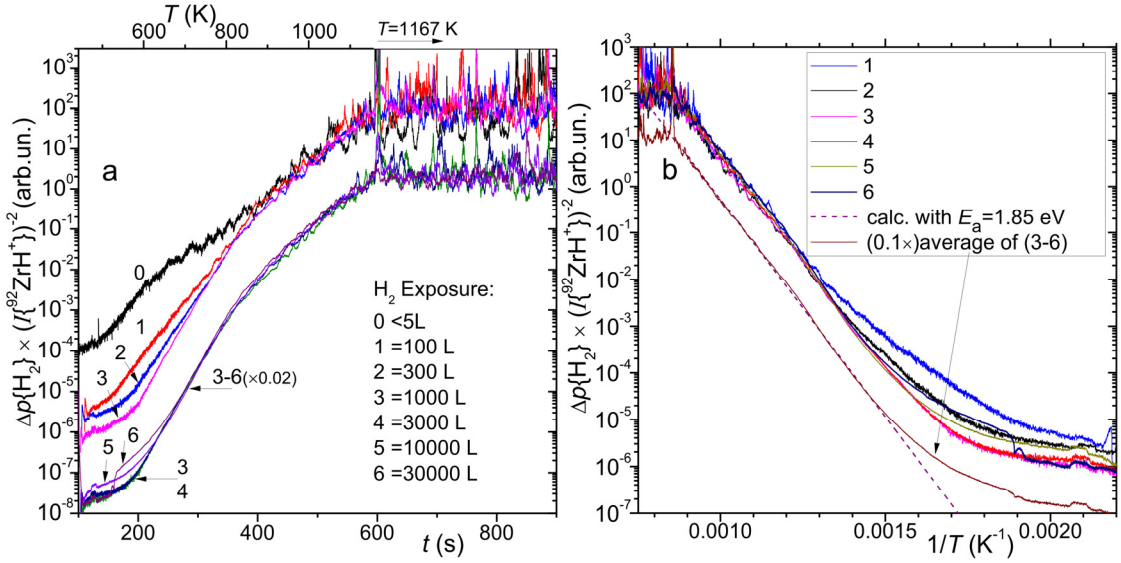

Figure 7. Dependences of the ratio of desorbing hydrogen pressure (from Fig.6b) to hydrogen-containing secondary ion emission intensity $I\{^{92}ZrH^+\}$ squared (from Fig.6a) on the sample heating/desorption time (**a**) and on the inverse sample temperature (**b**). Note that some dependence curves are manually shifted on Y-scale for better visibility.

4. CONCLUSIONS

The developed model is a simple and useful tool for practical analysis and characterization of hydrogen interaction processes with metal samples using the dynamic SIMS technique as demonstrated by the examples of extraction of the quantitative process parameters of hydrogen sputtering, absorption, and desorption. At the same time, the simplified reflection of the processes, characteristic parameters of which often depend on the amount of coverage, can limit the model's applicability. Regardless of that, in the case of analysis of SIMS measurements, the major obstacle preventing the full-potential realization of the model capabilities to quantitatively characterize the interaction processes occurring during the experiments was the lack of experimental data on the exact correspondence of the yields of secondary ions to the hydrogen concentration on the surface and the yields nonlinearities, which is a problem of the experimental technique rather than of the model and should be addressed in future studies.

ORCID

Ivan I. Okseniuk, https://orcid.org/0000-0002-8139-961X; **Viktor O. Litvinov**, https://orcid.org/0000-0003-2311-2817
Inna O. Afanasieva, https://orcid.org/0000-0002-9523-9780; **Dmytro I. Shevchenko**, https://orcid.org/0000-0002-4556-039X
Valentyn V. Bobkov, https://orcid.org/0000-0002-6772-624X

Acknowledgments

The developments described in this paper are a preparatory work for the EURIZON project, which is funded by the European Union under grant agreement No.871072.

REFERENCES

[1] Z. Zhu, V. Shutthanandan, and M. Engelhard, "An investigation of hydrogen depth profiling using ToF-SIMS", Surface and Interface Analysis, **44**(2), 232–237 (2012). https://doi.org/10.1002/sia.3826

[2] F.A. Stevie, "Analysis of hydrogen in materials with and without high hydrogen mobility", Surface and Interface Analysis, **48**(5), 310–314 (2016). https://doi.org/10.1002/sia.5930

[3] S. Pal, J. Barrirero, M. Lehmann, Q. Jeangros, N. Valle, F.-J. Haug, A. Hessler-Wyser, C.N. Shyam Kumar, F. Mücklich, T. Wirtz, and S. Eswara, "Quantification of hydrogen in nanostructured hydrogenated passivating contacts for silicon photovoltaics combining SIMS-APT-TEM: A multiscale correlative approach", Applied Surface Science, **555**, 149650 (2021). https://doi.org/10.1016/j.apsusc.2021.149650

[4] M. Riedel, and H. Düsterhöft, "Hydrogen outgassing of ZrNiCu(H) amorphous alloy studied by secondary ion mass spectrometry", Rapid Communications in Mass Spectrometry, **12**(20), 1510–1514 (1998). https://doi.org/10.1002/(SICI)1097-0231(19981030)12:20<1510::AID-RCM334>3.0.CO;2-2
[5] A. Nishimoto, M. Koyama, S. Yamato, Y. Oda, T. Awane, and H. Noguchi, "Detection of Charged Hydrogen in Ferritic Steel through Cryogenic Secondary Ion Mass Spectrometry", ISIJ International, **55**(1), 335–337 (2015). https://doi.org/10.2355/isijinternational.55.335
[6] T. Asakawa, D. Nagano, S. Denda, and K. Miyairi, "Influence of primary ion beam irradiation conditions on the depth profile of hydrogen in tantalum film", Applied Surface Science, **255**(4), 1387–1390 (2008). https://doi.org/10.1016/j.apsusc.2008.05.042
[7] X. Lin, A. Fucsko, K. Noehring, E. Gabriel, A. Regner, S. York, and D. Palsulich, "New SIMS method to characterize hydrogen in polysilicon films", Journal of Vacuum Science & Technology B, **40**(1), (2022). https://doi.org/10.1116/6.0001472
[8] J. Sameshima, and S. Numao, "Behavior and process of background signal formation of hydrogen, carbon, nitrogen, and oxygen in silicon wafers during depth profiling using dual-beam TOF-SIMS", Surface and Interface Analysis, **54**(2), 165–173 (2022). https://doi.org/10.1002/sia.7035
[9] D. Andersen, H. Chen, S. Pal, L. Cressa, O. De Castro, T. Wirtz, G. Schmitz, and S. Eswara, "Correlative high-resolution imaging of hydrogen in Mg2Ni hydrogen storage thin films", International Journal of Hydrogen Energy, **48**(37), 13943–13954 (2023). https://doi.org/10.1016/j.ijhydene.2022.12.216
[10] M.V. Lototskyy, B.P. Tarasov, and V.A. Yartys, "Gas-phase applications of metal hydrides", Journal of Energy Storage, **72**, 108165 (2023). https://doi.org/10.1016/j.est.2023.108165
[11] V.A. Litvinov, I.I. Okseniuk, D.I. Shevchenko, and V.V. Bobkov, "Secondary-ion mass spectrometry study of LaNi5-hydrogen-oxygen system", Ukrainian Journal of Physics, **66**(8), 723–735 (2021). https://doi.org/10.15407/ujpe66.8.723
[12] I. Okseniuk, and D. Shevchenko, "SIMS studies of hydrogen interaction with the TiFe alloy surface: hydrogen influence on secondary ion yields", Surface Science, **716**, 121963 (2022). https://doi.org/10.1016/j.susc.2021.121963
[13] I.I. Okseniuk, V.O. Litvinov, D.I. Shevchenko, R.L. Vasilenko, S.I. Bogatyrenko, and V.V. Bobkov, "Hydrogen interaction with Zr-based getter alloys in high vacuum conditions: In situ SIMS-TPD studies", Vacuum, **197**, 110861 (2022). https://doi.org/10.1016/J.VACUUM.2021.110861
[14] V.A. Litvinov, I.I. Okseniuk, D.I. Shevchenko, and V. V. Bobkov, "SIMS Study of Hydrogen Interaction with the LaNi5 Alloy Surface", Journal of Surface Investigation, **12**(3), 576–583 (2018). https://doi.org/10.1134/S1027451018030321
[15] V.O. Litvinov, I.I. Okseniuk, D.I. Shevchenko, and V. V. Bobkov, "The Role of Surface in Hydride Formation Processes", East European Journal of Physics, (3), 10–42 (2023). https://doi.org/10.26565/2312-4334-2023-3-01
[16] C.S. Zhang, B. Li, and P.R. Norton, "The study of hydrogen segregation on Zr(0001) and Zr(1010) surfaces by static secondary ion mass spectroscopy, work function, Auger electron spectroscopy and nuclear reaction analysis", Journal of Alloys and Compounds, **231**(1–2), 354–363 (1995). https://doi.org/10.1016/0925-8388(95)01847-6
[17] X.Y. Zhu, and J.M. White, "Hydrogen interaction with nickel(100): a static secondary ion mass spectroscopy study", The Journal of Physical Chemistry, **92**(13), 3970–3974 (1988). https://doi.org/10.1021/j100324a056
[18] A. Benninghoven, P. Beckmann, D. Greifendorf, K.H. Müller, and M. Schemmer, "Hydrogen detection by secondary ion mass spectroscopy: Hydrogen on polycrystalline nickel", Surface Science, **107**(1), 148–164 (1981). https://doi.org/10.1016/0039-6028(81)90618-X
[19] T. Asakawa, D. Nagano, H. Miyazawa, and I. Clark, "Absorption, discharge, and internal partitioning behavior of hydrogen in the tantalum and tantalum oxide system investigated by in situ oxidation SIMS and ab initio calculations", Journal of Vacuum Science & Technology B, **38**(3), 034008 (2020). https://doi.org/10.1116/6.0000100
[20] A. Röhsler, O. Sobol, H. Hänninen, and T. Böllinghaus, "In-situ ToF-SIMS analyses of deuterium re-distribution in austenitic steel AISI 304L under mechanical load", Scientific Reports, **10**(1), 3611 (2020). https://doi.org/10.1038/s41598-020-60370-2
[21] P. Kesten, A. Pundt, G. Schmitz, M. Weisheit, H.U. Krebs, and R. Kirchheim, "H- and D distribution in metallic multilayers studied by 3-dimensional atom probe analysis and secondary ion mass spectrometry," *Journal of Alloys and Compounds*, (2002), pp. 225–228. https://doi.org/10.1016/S0925-8388(01)01596-1
[22] C.S. Zhang, B. Li, and P.R. Norton, "The initial stages of interaction of hydrogen with the Zr(10$\bar{1}$0) surface", Surface Science, **346**(1–3), 206–221 (1996). https://doi.org/10.1016/0039-6028(95)00904-3
[23] J. Ekar, P. Panjan, S. Drev, and J. Kovač, "ToF-SIMS Depth Profiling of Metal, Metal Oxide, and Alloy Multilayers in Atmospheres of H 2 , C 2 H 2 , CO, and O 2", Journal of the American Society for Mass Spectrometry, **33**(1), 31–44 (2022). https://doi.org/10.1021/jasms.1c00218
[24] J. Ekar, and J. Kovač, "AFM Study of Roughness Development during ToF-SIMS Depth Profiling of Multilayers with a Cs + Ion Beam in a H 2 Atmosphere", Langmuir, **38**(42), 12871–12880 (2022). https://doi.org/10.1021/acs.langmuir.2c01837
[25] J. Ekar, S. Kos, and J. Kovač, "Quantitative Aspects of ToF-SIMS Analysis of Metals and Alloys in a UHV, O2 and H2 Atmosphere", Preprint (at https://www.ssrn.com), (2024). https://doi.org/10.2139/ssrn.4683611
[26] O.B. Malyshev, *Vacuum in Particle Accelerators* (Wiley, 2019)
[27] I. Sereda, Y. Hrechko, I. Babenko, and M. Azarenkov, "The emission of H− ions from Penning-type ion source with metal hydride cathode in pulsating regime", Vacuum, **200**, 111006 (2022). https://doi.org/10.1016/j.vacuum.2022.111006
[28] I. Sereda, Y. Hrechko, I. Babenko, and M. Azarenkov, "The Features of Intense Electron Flow Impact on Metal Hydride Electrode", East European Journal of Physics, (2), 99–102 (2022). https://doi.org/10.26565/2312-4334-2022-2-12
[29] I. Sereda, Y. Hrechko, and I. Babenko, "The Plasma Parameters of Penning Discharge with Negatively Biased Metal Hydride Cathode at Longitudinal Emission of H– Ions", East European Journal of Physics, (3), 81–86 (2021). https://doi.org/10.26565/2312-4334-2021-3-12
[30] E.A. Hodille, S. Markelj, M. Pecovnik, M. Ajmalghan, Z.A. Piazza, Y. Ferro, T. Schwarz-Selinger, and C. Grisolia, "Kinetic model for hydrogen absorption in tungsten with coverage dependent surface mechanisms", Nuclear Fusion, **60**(10), 106011 (2020). https://doi.org/10.1088/1741-4326/aba454
[31] K.E. Lu, and R.R. Rye, "Flash desorption and equilibration of H2 and D2 on single crystal surfaces of platinum", Surface Science, **45**(2), 677–695 (1974). https://doi.org/10.1016/0039-6028(74)90197-6

[32] V.A. Litvinov, I.I. Okseniuk, D.I. Shevchenko, and V. V. Bobkov, "SIMS study of the surface of lanthanum-based alloys", Ukrainian Journal of Physics, **62**(10), 845–857 (2017). https://doi.org/10.15407/ujpe62.10.0845
[33] V.T. Cherepin, M.O. Vasylyev, I.M. Makeeva, V.M. Kolesnik, and S.M. Voloshko, "Secondary Ion Emission during the Proton Bombardment of Metal Surfaces", Uspehi Fiziki Metallov, **19**(1), 49–69 (2018). https://doi.org/10.15407/ufm.19.01.049
[34] A. Wucher, "Formation of atomic secondary ions in sputtering", Applied Surface Science, **255**(4), 1194–1200 (2008). https://doi.org/10.1016/j.apsusc.2008.05.252
[35] K. Christmann, "Adsorption of Hydrogen," in *Surface and Interface Science, Volume 5 and 6: Volume 5 - Solid Gas Interfaces I; Volume 6 - Solid Gas Interfaces II*, edited by K. Wandelt, (John Wiley & Sons, 2016), pp. 255–357
[36] J. Sopka, and H. Oechsner, "Determination of hydrogen concentration depth profiles in a-Si:H by Secondary Neutral Mass Spectrometry (SNMS)", Journal of Non-Crystalline Solids, **114**, 208–210 (1989). https://doi.org/10.1016/0022-3093(89)90115-4
[37] J. Scholz, H. Züchner, H. Paulus, and K.-H. Müller, "Ion bombardment induced segregation effects in VDx studied by SIMS and SNMS", Journal of Alloys and Compounds, **253**–**254**, 459–462 (1997). https://doi.org/10.1016/S0925-8388(96)03000-9
[38] D.N. Denzler, C. Frischkorn, C. Hess, M. Wolf, and G. Ertl, "Electronic Excitation and Dynamic Promotion of a Surface Reaction", Physical Review Letters, **91**(22), 226102 (2003). https://doi.org/10.1103/PhysRevLett.91.226102
[39] F. Le Pimpec, O. Gröbner, and J.M. Laurent, "Electron stimulated molecular desorption of a non-evaporable Zr–V–Fe alloy getter at room temperature", Nuclear Instruments and Methods in Physics Research Section B: Beam Interactions with Materials and Atoms, **194**(4), 434–442 (2002). https://doi.org/10.1016/S0168-583X(02)01034-0
[40] Y. Kudriavtsev, R. Asomoza, A. Hernandez, D.Y. Kazantsev, B.Y. Ber, and A.N. Gorokhov, "Nonlinear effects in low-energy ion sputtering of solids", Journal of Vacuum Science & Technology A, **38**(5), 053203 (2020). https://doi.org/10.1116/6.0000262
[41] V. V Ovchinnikov, F.F. Makhin'ko, and V.I. Solomonov, "Thermal-spikes temperature measurement in pure metals under argon ion irradiation (E = 5-15 keV)", Journal of Physics: Conference Series, **652**, 012070 (2015). https://doi.org/10.1088/1742-6596/652/1/012070
[42] L.O. Williams, *Hydrogen Power: An Introduction to Hydrogen Energy and Its Applications* (Pergamon press, 2013)
[43] K. Christmann, "Interaction of hydrogen with solid surfaces", Surface Science Reports, **9**(1–3), 1–163 (1988). https://doi.org/10.1016/0167-5729(88)90009-X
[44] G. Ross, "Analysis of hydrogen isotopes in materials by secondary ion mass spectrometry and nuclear microanalysis", Vacuum, **45**(4), 375–387 (1994). https://doi.org/10.1016/0042-207X(94)90306-9
[45] M. Wilde, M. Matsumoto, L. Gao, T. Schwarz-Selinger, A. Manhard, and W. Jacob, "Cross section of 15N-2D nuclear reactions from 3.3 to 7.0 MeV for simultaneous hydrogen and deuterium quantitation in surface layers with 15N ion beams", Nuclear Instruments and Methods in Physics Research Section B: Beam Interactions with Materials and Atoms, **478**, 56–61 (2020). https://doi.org/10.1016/j.nimb.2020.05.020
[46] M. Wilde, S. Ohno, S. Ogura, K. Fukutani, and H. Matsuzaki, "Quantification of Hydrogen Concentrations in Surface and Interface Layers and Bulk Materials through Depth Profiling with Nuclear Reaction Analysis", Journal of Visualized Experiments, (109), (2016). https://doi.org/10.3791/53452
[47] V.P. Zhdanov, "Arrhenius parameters for rate processes on solid surfaces", Surface Science Reports, **12**(5), 185–242 (1991). https://doi.org/10.1016/0167-5729(91)90011-L
[48] H.J. Kreuzer, S.H. Payne, and Y.K. Tovbin, "Equilibria and Dynamics of Gas Adsorption on Heterogeneous Solid Surfaces," in *Studies in Surface Science and Catalysis*, edited by G.Z. Edited by W. Rudziński, W.A. Steele, (Elsevier, 1997), pp. 153–284
[49] K. Christmann, "Kinetics, energetics and structure of hydrogen adsorbed on transition metal single crystal surfaces", Bulletin Des Sociétés Chimiques Belges, **88**(7–8), 519–539 (2010). https://doi.org/10.1002/bscb.19790880706
[50] D.L.S. Nieskens, A.P. van Bavel, and J.W. Niemantsverdriet, "The analysis of temperature programmed desorption experiments of systems with lateral interactions; implications of the compensation effect", Surface Science, **546**(2–3), 159–169 (2003). https://doi.org/10.1016/j.susc.2003.09.035
[51] K. Christmann, O. Schober, G. Ertl, and M. Neumann, "Adsorption of hydrogen on nickel single crystal surfaces", The Journal of Chemical Physics, **60**(11), 4528–4540 (1974). https://doi.org/10.1063/1.1680935

ПРОСТА АНАЛІТИЧНА МОДЕЛЬ ПОКРИТТЯ ПОВЕРХНІ ВОДНЕМ ПІД ВПЛИВОМ РІЗНИХ ПРОЦЕСІВ НА ПОВЕРХНІ ТА ІОННОГО БОМБАРДУВАННЯ

Іван І. Оксенюк, Віктор О. Літвінов, Дмитро І. Шевченко, Інна О. Афанасьєва, Валентин В. Бобков
Харківський національний університет імені В. Н. Каразіна, майдан Свободи 4, 61022, Харків, Україна

У статті описано просту аналітичну модель, яка дозволяє розрахувати покриття поверхні воднем під дією декількох процесів, що можуть відбуватися одночасно під час бомбардування/розпилення поверхні зразка іонним пучком, зокрема під час аналізу за допомогою вторинної іонної мас-спектрометрії (ВІМС). Модель розглядає процеси дисоціативної адсорбції, десорбції, поглинання з поверхні в об'єм зразка та видалення водню іонним бомбардуванням. Після опису моделі наведено низку прикладів її практичного застосування для інтерпретації експериментальних результатів, отриманих під час *in situ* ВІМС-досліджень взаємодії водню з гідридоутворюючими сплавами, TiFe, Zr_2Fe та з нікелем. У наведених прикладах, із застосуванням різних апроксимацій моделі було успішно визначено низку кількісних характеристик поверхневих процесів за участю водню, зокрема швидкість розпилення водню, величини енергії активації десорбції та абсорбції водню.

Ключові слова: *вторинна іонна мас-спектрометрія; іонне бомбардування; розпилення; накопичення водню; адсорбція; десорбція; кінетика*